

An analysis of the performance of coupled cluster methods for core excitations and core ionizations using standard basis sets

Johanna P. Carbone

*Dipartimento di Scienze Chimiche e Farmaceutiche,
Università degli Studi di Trieste, I-34127, Trieste, Italy*

Lan Cheng

*Department of Chemistry, Krieger School of Arts and Sciences,
Johns Hopkins University, Baltimore, MD 21218, USA*

Rolf H. Myhre

Department of Chemistry, Norwegian University of Science and Technology, N-7491 Trondheim, Norway

Devin Matthews

*Institute for Computational Engineering and Sciences,
University of Texas at Austin, Austin, TX 78712, USA*

Henrik Koch

*Department of Chemistry, Norwegian University of Science and Technology, N-7491 Trondheim, Norway and
Scuola Normale Superiore, Pisa, Italy*

Sonia Coriani*

Department of Chemistry, Technical University of Denmark, DK-2800 Kgs. Lyngby, Denmark

An extensive analysis has been carried out of the performance of standard families of basis sets with the hierarchy of coupled cluster methods CC2, CCSD, CC3 and CCSDT in computing selected Oxygen, Carbon and Nitrogen K-edge (vertical) core excitation and ionization energies within a core-valence separated scheme in the molecules water, ammonia, and carbon monoxide. Complete basis set limits for the excitation energies have been estimated via different basis set extrapolation schemes. The importance of scalar relativistic effects has been established within the spin-free exact two-component theory in its one-electron variant (SFX2C-1e).

* Corresponding author. Email: soco@kemi.dtu.dk

I. INTRODUCTION

Core-level spectroscopy, including techniques such as Near-Edge Absorption Fine Structure and X-ray Photoelectron spectroscopies, is widely used in various areas of contemporary research, such as in surface science, organic electronics, and medical biological research [1]. It is considered a powerful tool to gain insight into the electronic structure of molecular species. The recent improvements of the synchrotron radiation sources and the emergence of the free-electron laser have further broadened the range of phenomena and systems that can be studied by core-level spectroscopy, see e.g. Refs.[1–9]. An essential requirement for a successful application of core-level techniques is the availability of reliable computational methods that allow for a proper interpretation of the resulting spectra. Several quantum chemical approaches exist for the calculation of core-excited/ionized states. While referring to Ref. 10 for a recent review, we mention here as examples the symmetry-adapted cluster configuration interaction (SAC-CI) [11], the GW approximation (self-energy approximated by Green-function G and screened Coulomb W) to the Bethe–Salpeter equation [12, 13], the static-exchange (STEX) approach [14], and the restricted and unrestricted algebraic diagrammatic construction scheme (ADC) [15–18] up to third order exploiting the core–valence separation (CVS) [19] approximation. Large systems are often treated with time-dependent density functional theory (TD-DFT) [20–26], but the results are plagued by the self-interaction error and the arbitrary dependence on the choice of the exchange–correlation functional. Indeed, unless short-range corrected hybrid functionals are used [27], core-excited states calculated by TD-DFT with conventional functionals often reproduce experimental spectra qualitatively well, but the self-interaction error and the small gap between occupied and unoccupied electronic levels inherent in the TD-DFT formalism lead to underestimation of core-excited states. Therefore absolute core excitation energies obtained by conventional TD-DFT are typically corrected by shifting them tens of eVs in order to agree with experiment. Among the time-independent DFT-based approaches for core excitations, we mention the recently proposed, and remarkably accurate, variational orthogonality constrained density functional theory method of Evangelista and co-workers [28, 29], see also the work of Glushkov, Assfeld and coworkers on orthogonality constrained/local Hartree-Hock Self-Consistent-Field [30–33]. Over the last eight years, we have made a significant effort to extend the applicability of the coupled cluster linear response (CC-LR) [34, 35] and equation-of-motion coupled-cluster (EOM-CC) [36–38] formalisms to the computation of core-level spectro-

scopies [6, 39–49]. The CC ansatz is known to provide a systematic hierarchy of models with increasing accuracy, allowing for the prediction of molecular properties and spectra with controlled accuracy within the hierarchy [35, 50, 51].

With the introduction in 2015 of CVS and restricted-excitation-window schemes within CC-LR and EOM-CC [43, 44, 52], the use of CC methods for the determination of core-absorption spectra and core ionization energies has become as straightforward as it is for UV-vis excitations. Since the computational determination of spectroscopic observables related to the interaction of the sample with X-ray radiation displays strong dependence on the level of theory and size of the basis sets, a systematic approach becomes particularly attractive. An important component to this end is a rigorous assessment of the basis set requirements and the relative accuracy of the various CC approximations, when computing core spectra using the different members of the CC(-LR) hierarchy. This study is meant as a contribution in this direction, in the spirit of a similar study conducted within the ADC formalism [18].

II. METHODOLOGY AND COMPUTATIONAL DETAILS

Calculations of core excitation energies, oscillator strengths (in length gauge) and ionization energies (IE) have been performed for the hierarchy of CC methods: coupled cluster singles and approximate doubles (CC2), coupled cluster singles and doubles (CCSD), coupled cluster singles, doubles and approximate triples (CC3), and coupled cluster singles, doubles and triples (CCSDT). All methods are extensively described in the literature, see e.g. Refs. 53–59, and we refrain therefore from repeating their derivation here. We limit ourselves to draw the reader’s attention to Ref. 43 for the description of how the core-valence separation scheme used here has been implemented within CC-LR/CC-EOM, to Ref. 60 for a new, more efficient, implementation of CC3, and to Refs. 61, 62 for efficient implementation of the CCSDT method. Scalar-relativistic effects have been taken into account in the CCSDT using the spin-free exact two-component theory in its one-electron variant (SFX2C-1e)[63–65].

All calculations up to CC3 have been run with a development version of the Dalton code [66], whereas the CFOUR [67] code was used for the CCSDT core excitation and ionization energies, respectively. Accurate experimental equilibrium geometries were adopted for all three systems: R_e (CO) = 1.12832 Å for CO; R_e (NH) = 1.011 Å and $\alpha_{\text{HNH}} = 106.7^\circ$ for ammonia; R_e (OH) = 0.9570

\AA and $\alpha_{\text{HOH}} = 104.5^\circ$ for water.

III. RESULTS AND DISCUSSION

A. Excitation energies

We start our discussion with a detailed comparison of the computed excitation energy values using the different basis sets across the CC hierarchy and with respect to the experimentally derived values. To this end, we plot in Figs. 1 to 4 the trends within each basis set family and method for the considered excitation energies. We will focus our discussion primarily on core excitations that are individually resolved in the experimental spectra: the $1s \rightarrow 3s$ (a_1) and $1s \rightarrow 3p$ (b_2) transitions in water, the $1s \rightarrow \pi^*$ transition for both C and O of CO, and the first three core excitations in NH_3 . The third intense peak in the X-ray absorption spectrum of H_2O is known to originate from the overlap of core transition into a_1 and b_1 states and will be commented upon in Section III C. The full set of numerical values of the core-excitation energies is available on arXiv [68].

Within each series of correlation consistent (cc) basis sets (regular, single augmented and double augmented), we observe an almost monotonically-decreasing trend (towards the experimental value) while increasing the basis set cardinal number.

In the cc-pVDZ basis, the excitation energies are always overestimated, by 2 to 5 eV depending on the case, with respect to both the other members of the series and the experimental values. By further increasing the cardinal number, the differences within each series reduce to tenths or hundredths of an eV. In other words, any Dunning set of $X \geq 3$ is reasonably accurate, and the results are significantly improved by inclusion of the first level of augmentation. Double augmentation has moderate effects for the chosen core excitations.

For the $1s \rightarrow 3s(a_1)$ in water, for instance, the differences between the CCSD results obtained for $X=2$ (DZ) and $X=3$ (TZ) in the series cc-pVXZ are always of the order of 3 eV, and slightly lower than 2 eV for the cc-pCVXZ series, progressively reducing to tenths and hundredths of an eV when increasing X . With reference to the experimental value for the same excitation, the basis sets with $X=2$ overestimate the edge by ca. 3.5–4.5 eV (depending on the basis); for $X \geq 3$, the deviation is reduced to ca. 1.0–1.2 eV for the (x-aug-)cc-pVXZ sets, and to ca. 1.5–1.7 eV for the (singly and doubly augmented) cc-pCVXZ sets.

The trend observed for the first excitation is roughly the same also for the second one. However, for the third and fourth core excitations of water (third peak in the experimental spectrum), as well as any higher lying excitations of more diffuse/Rydberg character than those considered here, it becomes of paramount importance to include additional diffuse functions [39, 47?].

Among the Pople basis sets, the 6-311++G** set emerges as remarkably accurate in basically all cases (states and methods) despite its moderate size, as also previously observed for the ADC family of methods [17]. Use of Cartesian d functions is to be slightly preferred.

The CCSD model systematically overestimates all core excitation energies (roughly of the same amount for all excitations), allowing for a 'rigid-shift' correction. The CC2 core excitation energies tend to be smaller than the CCSD ones, and they can be both red-shifted and blue-shifted compared to their experimental counterparts. For the first excitation, they are, at first sight, also closer to the experimental value, but the peak separation is underestimated. As we will see in Section III C, this, together with the results for intensities, actually results in a poor comparison of the CC2 spectral profile with the experimental one, at least for the three systems considered here.

B. Extrapolation towards the complete basis set (CBS) limits

As observed in Section III A, the results in the cc basis sets show a monotonically decreasing behaviour when increasing the cardinal number. The cc basis sets are known to yield a systematic convergence towards the complete basis set limit for the correlation energy of the ground state, as well as for other molecular properties, and various extrapolation formulae have been proposed in the literature. Some of these formulae tend to overestimate the limit, and others to underestimate it. Inspired by the analysis performed by Wenzel et al. for the ADC hierarchies [17], we have considered whether two popular extrapolations formulas, namely the X^{-3} formula [69] and the exponential formula [70],

$$E_X = E_{\text{CBS}} + AX^{-3}; \tag{1}$$

$$E_X = E_{\text{CBS}} + Ae^{-(X-1)} + Be^{-(X-1)^2} \tag{2}$$

can be applied to obtain an estimate of the CBS values of the core excitation energies considered in this study. In Eqs. 1 and 2, E_{CBS} is the resulting estimated energy of the CBS limit, and E_X is the calculated energy using the basis with the cardinal number X .

The two formulas have been applied in different ways in the literature for different properties. One can fit directly the results of each basis set series, imposing the functional forms in Eq. 1. Alternatively, one can derive the CBS limits via either a two point strategy (on the X^{-3} formula) or three point strategy (on the exponential formula), using the energy values relative to the two (three) highest values of the cardinal numbers: $X = Q, 5$ for the two-point extrapolation, and $X=T, Q, 5$ for the three point extrapolation. In the following, we have considered both strategies.

Notice that in standard basis set extrapolation schemes [69, 70], the exponential and X^{-3} formulae apply to Hartree-Fock and correlation energies, respectively. Since a separation of the excitation energies into HF and correlation contributions are not straightforward, we apply the formulae directly to the computed excitation energies. It is also important to bear in mind that these extrapolation formulae are not rigorous expressions for the basis set dependence of energies, but serve as an estimate of the trend.

In Fig. 5 we show the results obtained for one selected basis set family, the aug-cc-pCVXZ one, for all four CC methods in the case of the water molecule. The trends observed for CO (both edges) and NH_3 are completely analogous and can be found in the document on the arXiv [68]. The CBS values obtained directly from the two points X^{-3} or three points exponential procedures are basically identical, and only marginally different from those obtained by fitting with the exponential regression over the entire series. This difference is slightly larger than what was observed by Wenzel et al. [17] for the ADC methods.

By fitting the results with a X^{-3} formula, on the other hand, we could not reproduce the behaviour of the excitation energies.

C. Spectral bands

For comparison and assignment of the experimental spectra, the intensities of the absorption bands are required, and they are here obtained from the computed oscillator strengths. The full set of oscillator strengths obtained for the different basis sets at the CC2 and CCSD levels are available on the arXiv.

Spectral simulations based on oscillator strengths for the molecules H_2O and NH_3 computed in the cc-pCVXZ, aug-cc-pCVXZ and d-aug-cc-pCVXZ bases are shown in Fig. 6, and 7. They were obtained using a Lorentzian broadening function with a half-width-half-maximum of 0.01 a.u.

For the first two transitions of water, the CCSD oscillator strengths are practically the same as soon as one set of augmenting functions is added, and little affected by variation of the cardinal number, the largest differences in the spectra being due to variations in the position of the peaks. The situation is quite different for the third peak, which results from the combination of two excitations and has Rydberg character: many basis sets are insufficiently diffuse to yield an accurate description of the oscillator strengths, which are strongly overestimated. Inspection of the symmetry of the excited states also reveals that the third and fourth excited states contributing to the third spectral band switch position energetically in the different basis sets. An efficient strategy to have a good representation of the third band on H₂O is to include Rydberg type functions, as done in Ref. [39]. The CC2 oscillator strengths are more erratic, showing a relative intensity of the peaks at large variance compared to the experimental one, even in the larger basis sets. The CC2 spectra at the O K-edge of H₂O are “compressed”, due to the underestimation of the separation between the bands, as it can be appreciated in Fig. 6.

For carbon in CO both the CCSD and the CC2 intensity of the first transition grows slightly within each series as the cardinal number increases. The intensity of the second transition is roughly constant, while large variations are observed for the intensities of the third peak, in particular at CC2 level. For Oxygen, the intense peak has similarly almost constant intensity for all bases at CCSD level, while in the CC2 case some variations are recorded around an average value lower than the CCSD value. The intensities of the second and third peak are extremely low for both methods, and in the CC2 case sometimes even lower than the limit of detection.

Finally, in the case of ammonia (see Fig. 7), at both levels relatively large variations in intensity are observed for the second state (the most intense transition) for the bases lacking diffuse functions, and almost constant values for the other Dunning series. The intensities of the first state are roughly constant with the exception of in the smallest bases, which yield slightly overestimated values. Regarding the third state, the intensity decreases in the singly augmented sets and is almost constant for the doubly augmented ones, an indication of the greater sensitivity of this state to the presence of diffuse functions. The best agreement with the experimental profile is found for the d-aug-cc-pCVQZ basis set (we did not compute the aug-cc-pCV5Z and d-aug-cc-pCV5Z oscillator strengths). At CC2 level, there is in general a greater variation in the intensity, which is significantly smaller than in the CCSD case. Also at the N K-edge of NH₃, the peak separation is

underestimated, yielding “squeezed” spectral profiles, compared to both CCSD and experiment.

D. Ionization energies

Tables I and II contain the results of the core ionization energies for different basis sets in the CC hierarchy up to CCSDT.

TABLE I. Core ionization energies of water and ammonia using different standard basis sets and the hierarchy of CC methods CC2, CCSD, CC3 and CCSDT. Experimental values are 539.78 eV for H₂O and 405.6 eV for NH₃ [71].

Basis set	H ₂ O				NH ₃			
	CC2	CCSD	CC3	CCSDT	CC2	CCSD	CC3	CCSDT
VDZ	539.15	543.31	541.21	541.77	406.58	408.66	407.15	407.45
VTZ	537.56	540.67	538.54	539.04	404.65	406.30	404.69	404.90
VQZ	537.57	540.77	538.33	538.94	404.69	406.40	404.60	–
V5Z	537.55	540.85	538.25	–	404.70	406.49	404.59	–
CVDZ	539.15	542.70	540.46	540.97	406.07	408.16	406.50	406.76
CVTZ	537.92	541.14	538.90	539.40	405.05	406.82	405.12	405.33
CVQZ	537.91	541.26	538.76	–	405.04	406.89	405.04	–
CV5Z	537.90	541.35	538.70	–	405.04	406.95	–	–
aVDZ	539.88	544.08	541.31	542.31	406.59	409.01	407.24	407.71
aVTZ	537.61	541.00	538.49	539.23	404.70	406.51	404.72	405.02
aVQZ	537.59	540.91	538.31	539.02	404.71	406.49	404.61	404.89
aV5Z	537.56	540.89	538.24	–	404.71	406.52	–	–
aCVDZ	539.27	543.45	540.56	541.51	406.09	408.52	406.60	407.02
aCVTZ	537.98	541.47	538.87	539.61	405.10	407.03	405.17	405.47
aCVQZ	537.93	541.40	538.73	539.46	405.06	406.98	405.05	405.34
aCV5Z	537.91	541.38	538.69	–	405.05	406.97	–	–
6-311G	538.16	541.07	539.15	–	405.19	406.77	405.32	–
6-311G**	537.99	540.92	539.01	–	405.02	406.61	405.15	–
6-311++G**	538.09	541.46	538.97	–	405.09	406.92	405.19	–

Inspection of the results clearly reveals, also for the IE, the inaccuracy of the double zeta basis sets for the core IE: for all three edges (C, N and O) and at all CC levels the X=D basis sets overestimate the IEs by in between 1 to 3 eV. The largest improvement is observed for X=T, whereas going beyond triple- ζ has either moderate or negligible effect, and so also does the inclusion of single augmentation.

Moving along the CC hierarchy, we note that the CCSD IEs are significantly larger (1.5–4 eV)

TABLE II. Carbon monoxide. Core ionization energies of oxygen and carbon using different standard basis sets and the hierarchy of CC methods CC2, CCSD, CC3 and CCSDT. Experimental values are 296.2 eV for C and 542.5 eV for O [71].

Basis set	Carbon				Oxygen			
	CC2	CCSD	CC3	CCSDT	CC2	CCSD	CC3	CCSDT
VDZ	299.02	299.32	298.53	298.49	542.01	546.59	543.89	544.72
VTZ	297.17	296.98	295.99	295.88	539.92	543.71	541.19	541.83
VQZ	297.26	297.08	295.98	295.88	539.92	543.68	541.66	541.66
V5Z	297.27	297.12	–	–	539.89	543.67	–	–
CVDZ	298.46	298.81	297.80	297.73	541.40	545.97	543.14	543.91
CVTZ	297.64	297.54	296.48	296.38	540.28	544.18	541.55	542.19
CVQZ	297.65	297.59	296.44	296.34	540.25	544.18	–	–
CV5Z	297.66	297.61	–	–	540.24	544.18	–	–
aVDZ	299.04	299.34	298.49	298.46	542.16	546.83	543.98	543.93
aVTZ	297.20	297.04	296.00	295.90	539.96	543.79	541.18	541.86
aVQZ	297.28	297.11	295.999	295.90	539.94	543.71	541.02	541.68
aV5Z	297.29	297.14	–	–	539.90	543.69	–	–
aCVDZ	298.50	298.84	297.80	297.76	541.54	546.20	543.22	544.12
aCVTZ	297.68	297.62	296.53	296.43	540.32	544.27	541.57	542.25
aCVQZ	297.66	297.61	296.44	296.36	540.27	544.21	541.44	542.12
aCV5Z	297.66	297.62	–	–	540.25	544.19	–	–

than the CC2 ones for both O and N, whereas for the C K-edge they are just slightly smaller (a few tenths of eV). Inclusion of triple excitations at the approximate CC3 lowers the IEs by ≈ 2.5 – 2.8 eV for O, by ≈ 1.6 – 1.9 eV for N, and ≈ 1.0 eV for C. Inclusion of the full treatment of triples by CCSDT, on the other hand, increases the CC3 results by a constant amount (independent of the basis set) of ≈ 0.7 eV for the O edge, ≈ 0.3 eV for the N edge; the C-edge IEs, on the other hand, are further reduced by 0.1 eV.

Comparing with the experimental results, we observe that in the case of Carbon both CC2 and CCSD overestimate the IE; CC3 and CCSDT either overestimate or underestimate the IE, depending on the basis set, by a few tenths of eV.

The core IEs of the two types of oxygen K-edge (H_2O and CO) are significantly underestimated (ca 2 eV) at the CC2 level, and overestimated (1.5–2 eV) at the CCSD level. For $X \geq T$, the CC3 results are 1.0–1.5 eV lower than experiment. The CCSDT results in the largest core-valence set are about -0.3 eV from experiment (and relativistic effects are $+0.3$ eV).

The N-edge IE is underestimated by 0.5–1.0 eV at the CC2 level, and overestimated by 1.0–1.5

eV at the CCSD level. The CC3 estimates are very similar to the CC2 ones, and around -0.5 eV off in the core-valence bases. The agreement with experiment is further improved by full inclusion of triple excitations: in the aug-cc-pVQZ basis the CCSDT IE is -0.26 eV lower than the experimental IE.

The importance of scalar relativistic effects is illustrated in Table III. As previously observed [39, 46, 48], the relativistic effect is core-specific and practically the same independent of the chosen method and basis set. The effect is to increase the IEs in all cases, which can be ascribed to the contraction, and thereby stabilization, of the core orbitals.

TABLE III. Comparison of relativistic and non-relativistic results for the IEs (eV).

	Nonrel SFX2C-1e Δ Rel			Nonrel SFX2C-1e Δ Rel		
	O(H ₂ O)			N(NH ₃)		
CCSD/aVTZ	541.03	541.39	0.36	406.51	406.73	0.22
CCSD/aVQZ	540.91	541.30	0.39	406.50	406.71	0.21
CCSD/aV5Z	540.90	541.28	0.38	406.52	406.73	0.21
CCSD/aCVTZ	541.48	541.86	0.38	407.03	407.24	0.21
CCSD/aCVQZ	541.40	541.79	0.39	406.99	407.20	0.21
CCSD/aCV5Z	541.38	541.77	0.39	406.98	407.19	0.21
CCSDT/aVTZ	539.23	539.61	0.38	405.02	405.23	0.21
CCSDT/aVQZ	539.02	539.40	0.38	404.89	405.10	0.21
CCSDT/aCVTZ	539.61	540.00	0.39	405.47	405.68	0.21
CCSDT/aCVQZ	539.46	539.85	0.39	405.34	405.55	0.21
	O(CO)			C(CO)		
CCSD/aVTZ	543.79	544.17	0.38	297.04	297.14	0.10
CCSD/aVQZ	543.71	544.10	0.39	297.11	297.21	0.10
CCSD/aV5Z	543.69	544.07	0.38	297.14	297.24	0.10
CCSD/aCVTZ	544.27	544.65	0.38	297.62	297.72	0.10
CCSD/aCVQZ	544.21	544.59	0.38	297.61	297.71	0.10
CCSD/aCV5Z	544.19	544.57	0.38	297.62	297.72	0.10
CCSDT/aVTZ	541.86	542.25	0.39	295.90	295.99	0.09
CCSDT/aVQZ	541.68	542.06	0.38	295.90	295.99	0.09
CCSDT/aCVTZ	542.25	542.63	0.38	296.43	296.53	0.10
CCSDT/aCVQZ	542.12	542.50	0.38	296.36	296.46	0.10

IV. CONCLUDING REMARKS

We have carried out a coupled cluster investigation of the performance of the standard hierarchy CC2-CCSD-CC3-CCSDT in connection with conventional Dunning correlation-consistent and Pople basis sets to yield accurate vertical core excitation energies (and strengths) and core-ionization energies for N, C and O K-edges in the prototypical molecules H₂O, CO and NH₃. Complete basis set limit values have been derived.

The use of singly augmented triple-zeta basis sets is sufficiently accurate for the low-energy core excitations, which are of limited or no Rydberg character. The Pople set 6-311++G** set provides results of quality almost comparable as the aug-cc-pVTZ set, but at lower computational cost.

ACKNOWLEDGEMENTS

S.C. acknowledges financial support from the AIAS-COFUND program (Grant Agreement No. 609033) and from the Independent Research Fund Denmark, DFF-Forskningsprojekt2 (Grant No. 7014-00258B). H.K. acknowledges financial support from the FP7-PEOPLE-2013-IOF funding scheme (Project No. 625321) and a visiting professorship grant at DTU Chemistry from the Otto Mønsted Foundation. RHM acknowledges computer time from NOTUR through Project No. nn2962k. The COST Actions No. MP1306 “Modern Tools for Spectroscopy on Advanced Materials (EUSPEC)”, CM1204 “XUV/X-ray light and fast ions for ultrafast chemistry (XLIC)” and CM1405 “MOLIM–Molecules in Motion” are also acknowledged.

FIG. 1. H₂O, Oxygen K-edge. Basis set convergence of the first two vertical core excitation energies with

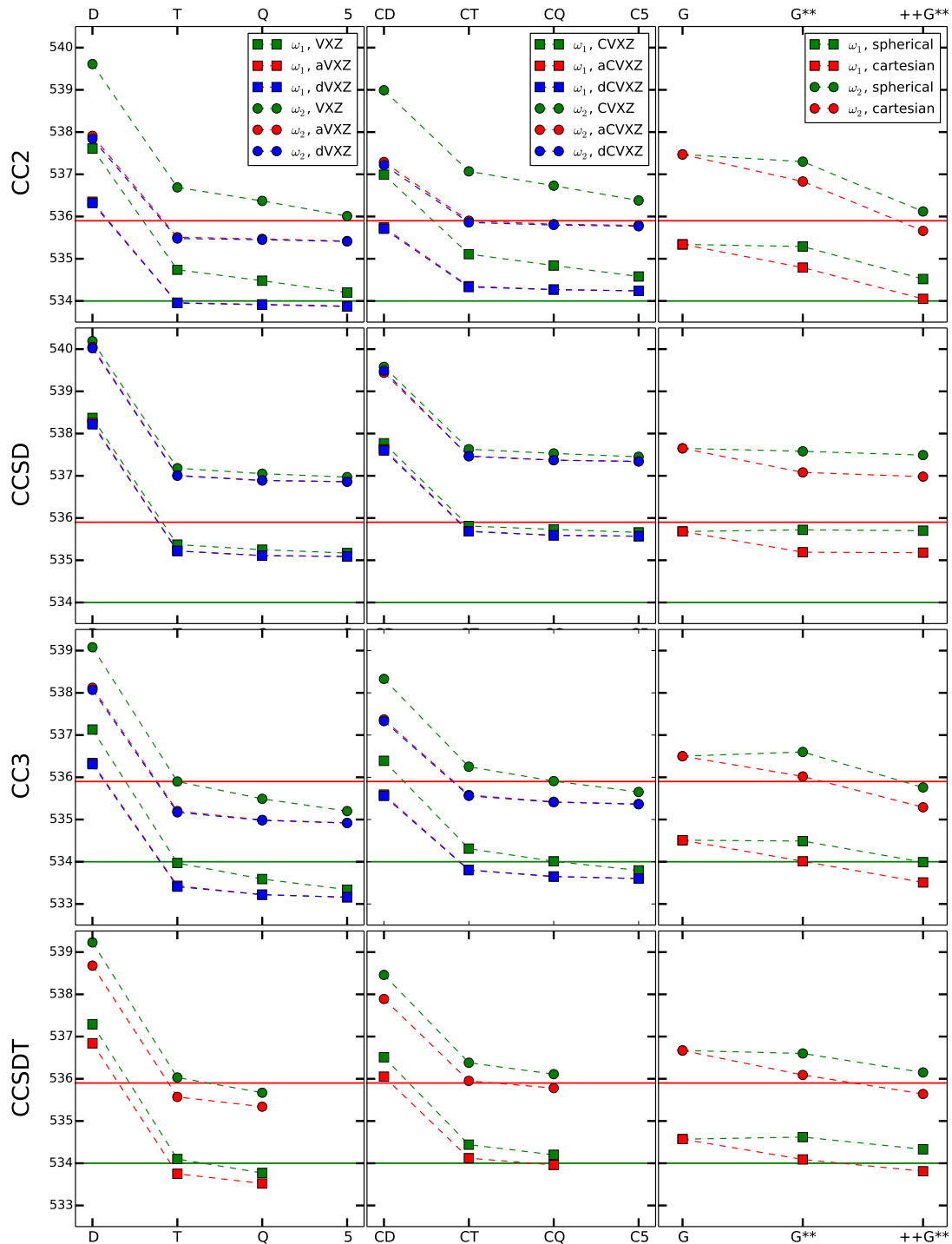


FIG. 2. CO, Carbon K-edge. Basis set convergence of the first two vertical core excitation energies with

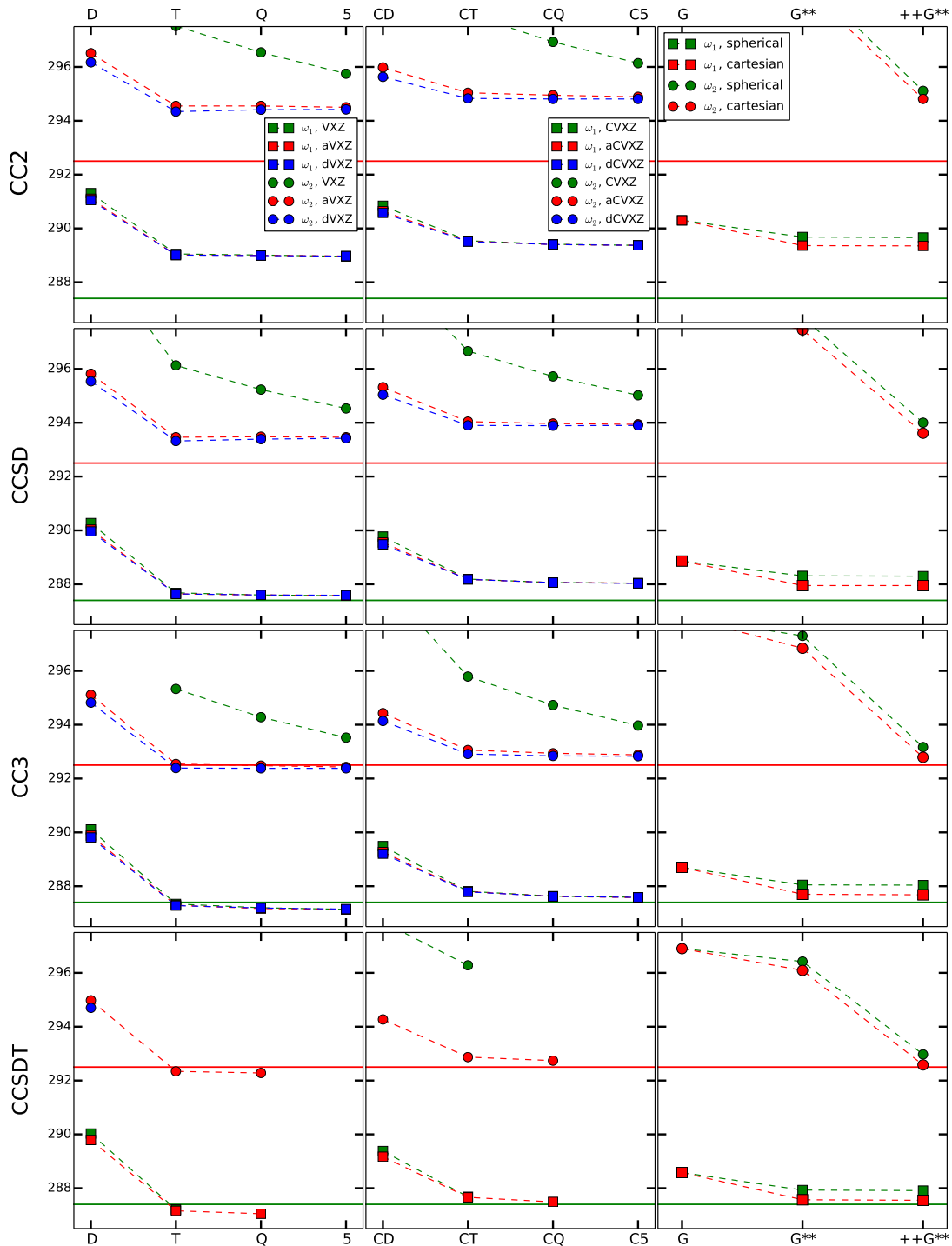


FIG. 3. CO, Oxygen K-edge. Basis set convergence of the first two vertical core excitation energies with

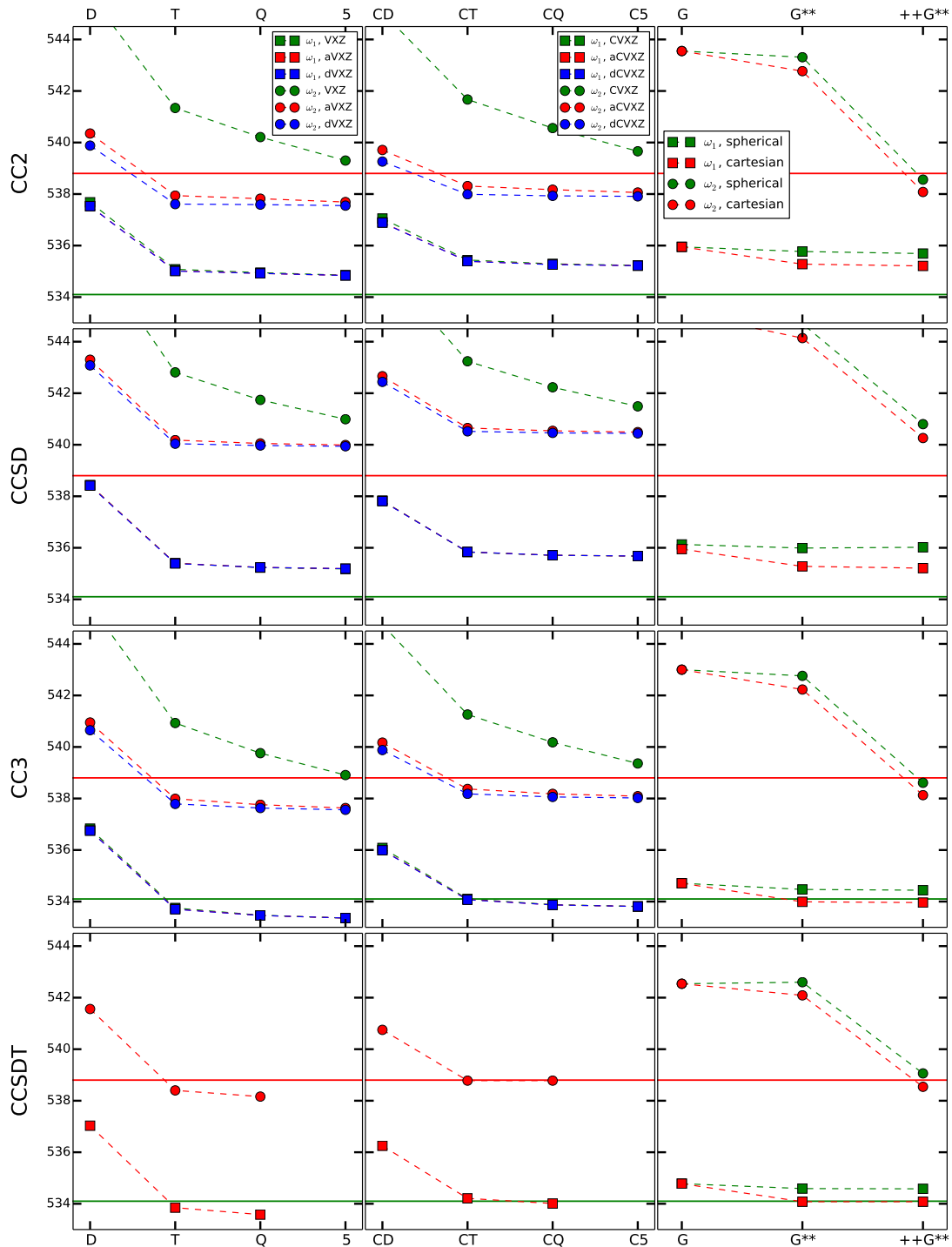


FIG. 4. NH_3 , Nitrogen K-edge. Basis set convergence of the first two vertical core excitation energies with

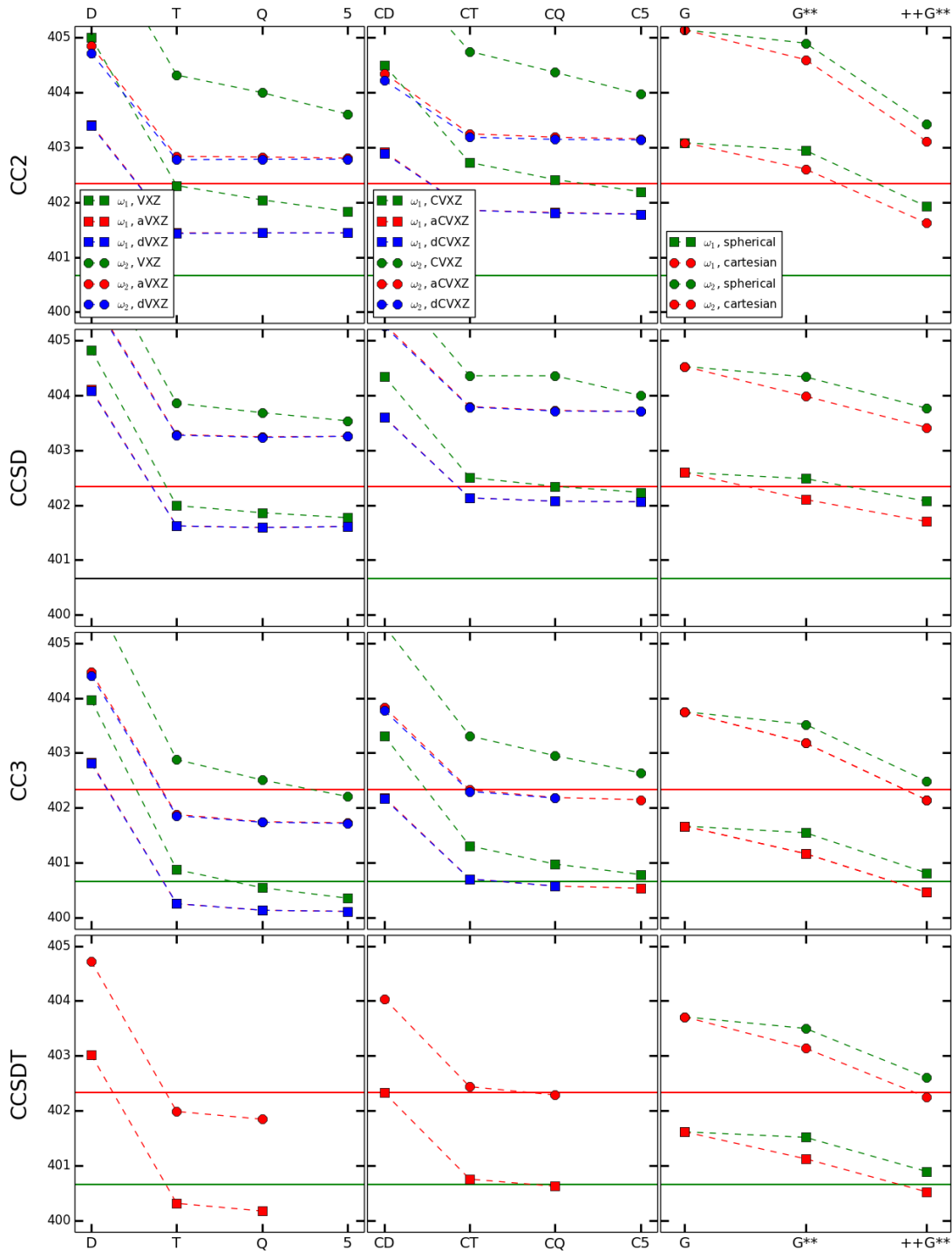


FIG. 5. H₂O, Oxygen K-edge. Extrapolated complete-basis set (CBS) limits for the first two core excitations with different CC methods and the aug-cc-pCVXZ series. Upper panels: CC2; middle panels: CCSD; Bottom panels: CC3. The horizontal green lines correspond to the experimentally estimated core energies.

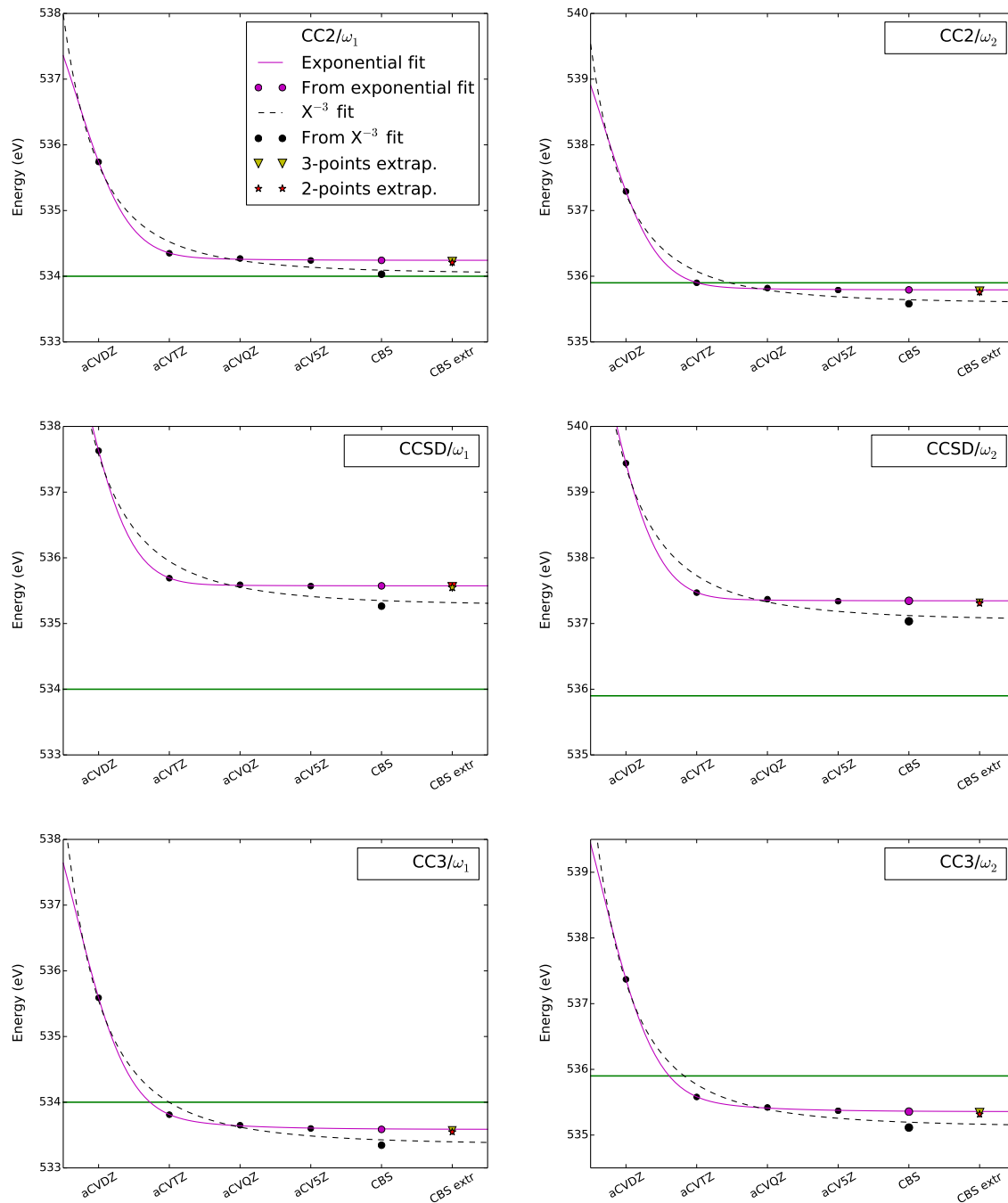


FIG. 6. H₂O, Oxygen K-edge. CC2 (left panels) and CCSD (right panels) spectral profiles with the x-aug-CVXZ basis sets. The augmented bases results are compared with the experimental spectrum [71], which has been shifted and rescaled to roughly overlap with the first computed band (X=T,Q,5).

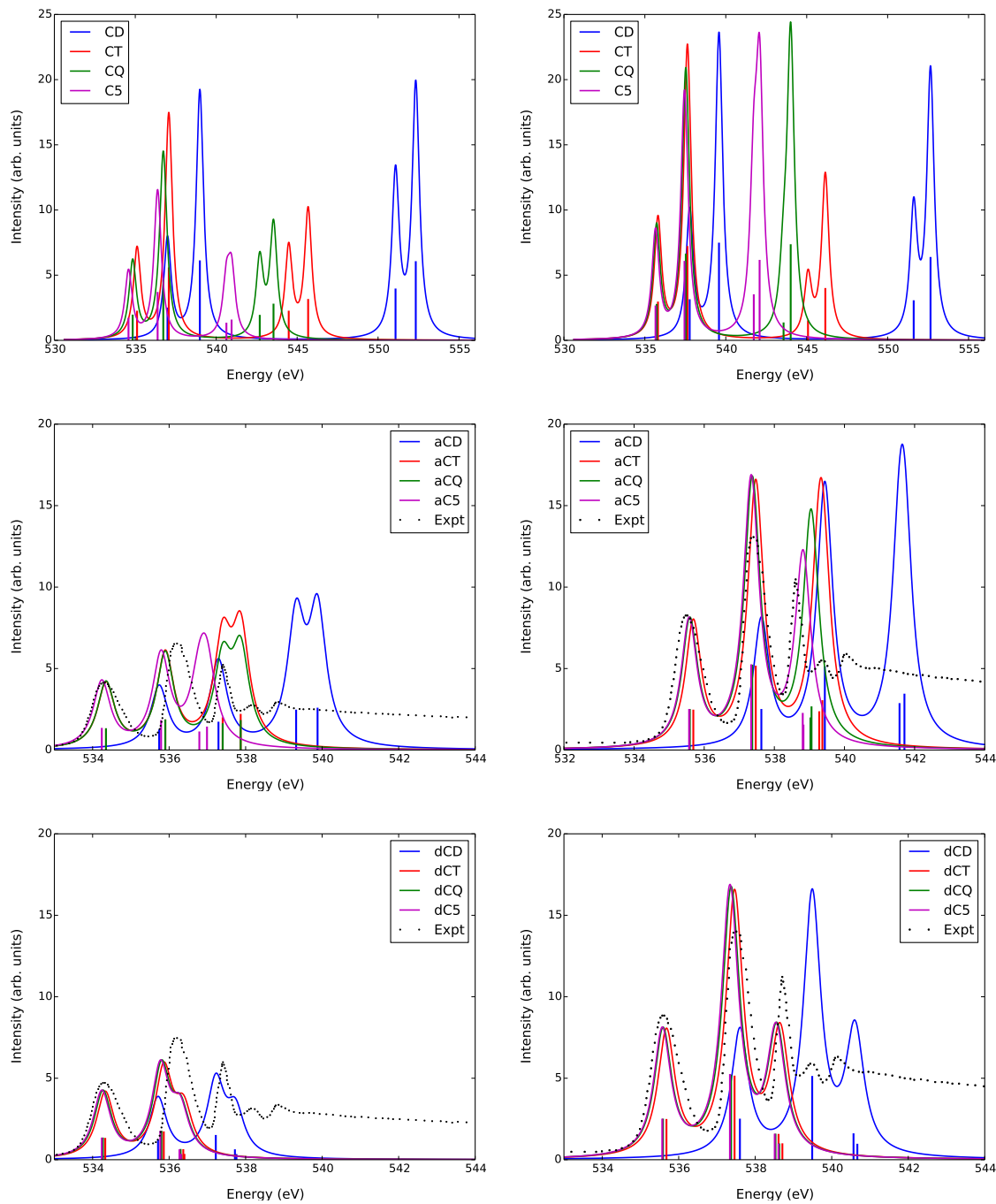
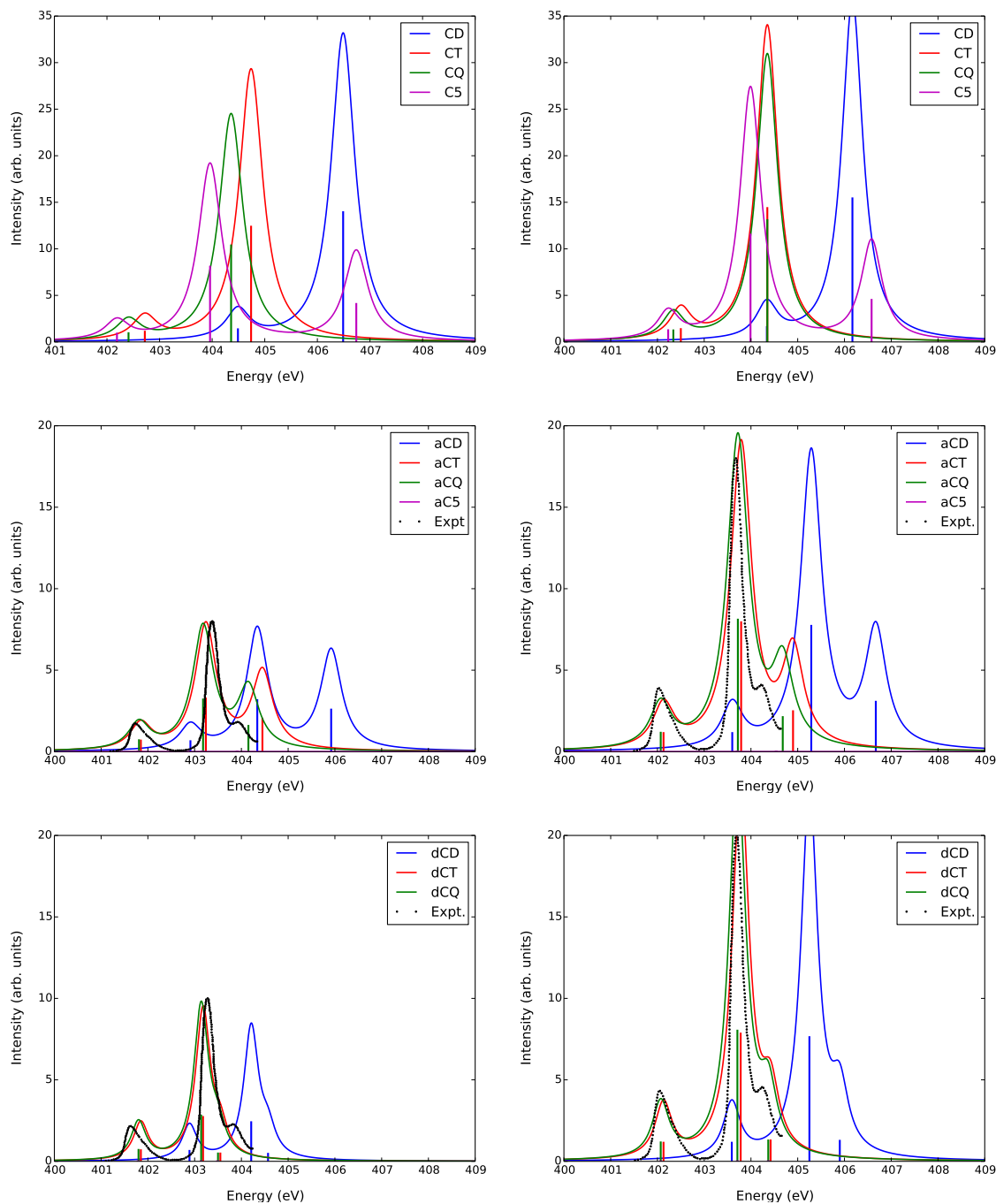


FIG. 7. NH_3 , Nitrogen K-edge. Spectral profiles (first 3 bands) at the CC2 (left) and CCSD (right) level in the cc-pCVXZ, aug-cc-pCVXZ and d-aug-cc-pCVXZ basis sets. The augmented bases results are compared with the experimental spectrum [71], which has been shifted and rescaled to roughly overlap with the first computed band ($X>D$).



-
- [1] *X-Ray Free Electron Lasers: Applications in Materials, Chemistry and Biology*; Bergmann, U., Yachandra, V., Yano, J., Eds.; Energy and Environment Series 18; Royal Society of Chemistry, 2017.
- [2] Van Kuiken, B. E.; Huse, N.; Cho, H.; Strader, M. L.; Lynch, M. S.; Schoenlein, R. W.; Khalil, M. J. *Phys. Chem. Lett.* **2012**, *3*, 1695–1700.
- [3] Piancastelli, M.; Simon, M.; Ueda, K. *J Electron Spectros Relat Phenomena* **2010**, *181*, 98–110.
- [4] Milne, C.; Penfold, T.; Chergui, M. *Coord. Chem. Rev.* **2014**, *277-278*, 44–68.
- [5] *X-Ray Absorption and X-ray Emission Spectroscopy; Theory and Applications*; van Bokhoven, J., Lamberti, C., Eds.; Wiley & Sons, 2016.
- [6] Wolf, T. et al. *Nature Commun.* **2017**, *8*, 1–7.
- [7] Chergui, M.; Collet, E. *Chem. Rev.* **2017**, *117*, 11025–11065.
- [8] Lin, F.; Liu, Y.; Yu, X.; Cheng, L.; Singer, A.; Shpyrko, O. G.; Xin, H. L.; Tamura, N.; Tian, C.; Weng, T. C.; Yang, X. Q.; Meng, Y. S.; Nordlund, D.; Yang, W.; Doeff, M. M. *Chem. Rev.* **2017**, *117*, 13123–13186.
- [9] Kraus, P. M.; Zürich, M.; Cushing, S. K.; Neumark, D. M.; Leone, S. R. *Nature Reviews Chemistry* **2018**, *2*, 82–94.
- [10] Norman, P.; Dreuw, A. *Chem. Rev.* **2018**, *118*, 7208–7248.
- [11] Kuramoto, K.; Ehara, M.; Nakatsuji, H. *J. Chem. Phys.* **2005**, *122*, 014304.
- [12] Vinson, J.; Rehr, J. J.; Kas, J. J.; Shirley, E. L. *Phys. Rev. B: Condens. Matter Mater. Phys.* **2011**, *83*, 115106.
- [13] Gilmore, K.; Vinson, J.; Shirley, E.; Prendergast, D.; Pemmaraju, C.; Kas, J.; Vila, F.; Rehr, J. *Computer Physics Communications* **2015**, *197*, 109–117.
- [14] Ågren, H.; Carravetta, V.; Vahtras, O.; Pettersson, M. L. G. *Theor. Chem. Acc.* **1997**, *97*, 14–40.
- [15] Schirmer, J. *Phys. Rev. A* **1982**, *26*, 2395–2416.
- [16] Dreuw, A.; Wormit, M. *WIREs Comput Mol Sci* **2015**, *5*, 82–95.
- [17] Wenzel, J.; Wormit, M.; Dreuw, A. *J. Comput. Chem.* **2014**, *35*, 1900.
- [18] Wenzel, J.; Holzer, A.; Wormit, M.; Dreuw, A. *J. Chem. Phys.* **2015**, *142*, 214104.
- [19] Cederbaum, L. S.; Domcke, W.; Schirmer, J. *Phys. Rev. A: At. Mol. Opt. Phys.* **1980**, *22*, 206–222.
- [20] Stener, M.; Fronzoni, G.; de Simone, M. *Chem. Phys. Lett.* **2003**, *15*, 115.
- [21] Ekström, U.; Norman, P.; Carravetta, V.; Ågren, H. *Phys. Rev. Lett.* **2006**, *97*, 143001.
- [22] Ekström, U.; Norman, P. *Phys. Rev. A* **2006**, *74*, 042722.
- [23] Tu, G.; Rinkevicius, Z.; Vahtras, O.; Ågren, H.; Ekström, U.; Norman, P.; Carravetta, V. *Phys. Rev. A* **2007**, *76*, 022506.

- [24] Liang, W.; Fischer, S. A.; Frisch, M. J.; Li, X. *J. Chem. Theory Comput.* **2011**, *7*, 3540–3547.
- [25] Besley, N. A.; Asmuruf, F. A. *Phys. Chem. Chem. Phys.* **2010**, *12*, 12024.
- [26] Lestrange, P. J.; Nguyen, P. D.; Li, X. *J. Chem. Theory Comput.* **2015**, *11*, 2994–2999.
- [27] Besley, N. A.; Gilbert, A. T.; Gill, P. M. *J. Chem. Phys.* **2009**, *130*, 124308.
- [28] Derricotte, W. D.; Evangelista, F. A. *Phys. Chem. Chem. Phys.* **2015**, *17*, 14360–14374.
- [29] Evangelista, F. A.; Shushkov, P.; Tully, J. C. *J. Phys. Chem. A* **2013**, *117*, 7378–7392.
- [30] Glushkov, V. N.; Assfeld, X. *Theor. Chem. Accounts* **2015**, *135*, 3.
- [31] Glushkov, V. N.; Assfeld, X. *J. Phys. B: At. Mol. Opt. Phys.* **2017**, *50*, 125101.
- [32] Ferré, N.; Assfeld, X. *J. Chem. Phys.* **2002**, *117*, 4119–4125.
- [33] Glushkov, V. N.; Assfeld, X. *J. Comp. Chem.* **2012**, *33*, 2058–2066.
- [34] Koch, H.; Jørgensen, P. *J. Chem. Phys.* **1990**, *93*, 3333–3344.
- [35] Christiansen, O.; Jørgensen, P.; Hättig, C. *Int. J. Quantum Chem.* **1998**, *98*, 1.
- [36] Stanton, J. F.; Bartlett, R. J. *J. Chem. Phys.* **1993**, *98*, 7029–7039.
- [37] Bartlett, R. J. *WIREs Comput. Mol. Sci.* **2012**, *2*, 126–138.
- [38] Krylov, A. I. *Ann. Rev. Phys. Chem.* **2008**, *59*, 433–462.
- [39] Coriani, S.; Christiansen, O.; Fransson, T.; Norman, P. *Phys. Rev. A* **2012**, *85*, 022507.
- [40] Coriani, S.; Fransson, T.; Christiansen, O.; Norman, P. *J. Chem. Theory Comput.* **2012**, *8*, 1616.
- [41] Fransson, T.; Coriani, S.; Christiansen, O.; Norman, P. *J. Chem. Phys.* **2013**, *138*, 124311.
- [42] List, N. H.; Coriani, S.; Kongsted, J.; Christiansen, O. *J. Chem. Phys.* **2014**, *141*, 244107.
- [43] Coriani, S.; Koch, H. *J. Chem. Phys.* **2015**, *143*, 181103.
- [44] Coriani, S.; Koch, H. *J. Chem. Phys.* **2016**, *145*, 149901.
- [45] Myhre, R. H.; Coriani, S.; Koch, H. *J. Chem. Theory Comput.* **2016**, *12*, 2633–2643.
- [46] Myhre, R. H.; Wolf, T. J.; Cheng, L.; Nandi, S.; Coriani, S.; Gühr, M.; Koch, H. *J. Chem. Phys.* **2018**, *148*, 064106.
- [47] Vidal, M. L.; Feng, X.; Epifanovsky, E.; Krylov, A. I.; Coriani, S. *J. Chem. Theory Comput.* **2019**, *15*, 3117.
- [48] Liu, J.; Matthews, D.; Coriani, S.; Cheng, L. *J. Chem. Theory and Comput.* **2019**, *15*, 1642–1651.
- [49] Faber, R.; Coriani, S. *J. Chem. Theory Comput.* **2019**, *15*, 520–528.
- [50] Helgaker, T.; Coriani, S.; Jørgensen, P.; Kristensen, K.; Olsen, J.; Ruud, K. *Chem. Rev.* **2012**, *112*, 543–631.
- [51] Helgaker, T.; Jørgensen, P.; Olsen, J. *Molecular Electronic Structure Theory*; Wiley, 2004.
- [52] Peng, B.; Lestrange, P. J.; Goings, J. J.; Caricato, M.; Li, X. *J. Chem. Theory Comput.* **2015**, *11*, 4146.
- [53] Christiansen, O.; Koch, H.; Jørgensen, P. *Chem. Phys. Lett.* **1995**, *243*, 409.
- [54] Purvis, G. D.; Bartlett, R. J. *J. Chem. Phys.* **1982**, *76*, 1910.

- [55] Koch, H.; Sánchez de Merás, A.; Helgaker, T.; Christiansen, O. *J. Chem. Phys.* **1996**, *104*, 4157.
- [56] Christiansen, O.; Koch, H.; Halkier, A.; Jørgensen, P.; Helgaker, T.; Sánchez de Merás, A. *J. Chem. Phys.* **1996**, *105*, 6921.
- [57] Koch, H.; Christiansen, O.; Jørgensen, P.; de Merás, A. S.; Helgaker, T. *J. Chem. Phys.* **1997**, *106*, 1808.
- [58] Christiansen, O.; Koch, H.; Jørgensen, P. *J. Chem. Phys.* **1995**, *103*, 7429–7441.
- [59] Kucharski, S. A.; Wloch, M.; Musiał, M.; Bartlett, R. J. *J. Chem. Phys.* **2001**, *115*, 8263–8266.
- [60] Myhre, R. H.; Koch, H. *J. Chem. Phys.* **2016**, *145*, 044111.
- [61] Matthews, D. A.; Stanton, J. F. *J. Chem. Phys.* **2015**, *142*, 064108.
- [62] Baraban, J. H.; Matthews, D. A.; Stanton, J. F. *J. Chem. Phys.* **2016**, *144*, 111102.
- [63] Dylla, K. G. *J. Chem. Phys.* **1997**, *106*, 9618–9626.
- [64] Liu, W.; Peng, D. *J. Chem. Phys.* **2009**, *131*, 031104.
- [65] Cheng, L.; Gauss, J. *J. Chem. Phys.* **2011**, *135*, 084114.
- [66] Aidas, K. et al. *WIREs Comput. Mol. Sci.* **2014**, *4*, 269.
- [67] Stanton, J. et al. *CFOUR, Coupled-Cluster techniques for Computational Chemistry*, 2015. <http://www.cfour.de/>.
- [68] Carbone, J. P.; Cheng, L.; Myhre, R. H.; Matthews, D.; Koch, H.; Coriani, S. *An analysis of the performance of coupled cluster methods for K-edge core excitations and ionizations using standard basis sets: Additional Tables and Figures.*, 2019.
- [69] Helgaker, T.; Klopper, W.; Koch, H.; Noga, J. *J. Chem. Phys.* **1997**, *106*, 9639.
- [70] Peterson, K. A.; Woon, D. E.; Dunning, T. H. *J. Chem. Phys.* **1994**, *100*, 7410–7415.
- [71] Schirmer, J.; Trofimov, A.; Randall, K.; Feldhaus, J.; Bradshaw, A. M.; Ma, Y.; Chen, C. T.; Sette, F. *Phys. Rev. A* **1993**, *47*, 1136.